# Closed-Loop Deep Neural Network-Based FES Control for Human Limb Tracking

Emily J. Griffis, Duc M. Le, Kimberly J. Stubbs, and Warren E. Dixon

Abstract—Functional electrical stimulation (FES) can be used as rehabilitative treatment for lost motor neuron function in people with neurological disorders. This paper considers a leg extension machine coupled to a participant for FES-induced closed-loop lower-limb tracking of a desired trajectory. FES-induced control faces challenges as the muscle dynamics exhibit nonlinear behaviors and have unstructured uncertainty. A closed-loop data-driven deep neural network (DNN)-based adaptive control method for FES-induced lower-limb position trajectory tracking is developed. A Lyapunov-based stability analysis is used to develop a closed-loop state-feedback adaptation law for the outer-layer weights of the DNN, which is combined with a feedback controller to yield semi-global asymptotic tracking.

#### I. INTRODUCTION

Functional electrical stimulation (FES) is a common rehabilitation technique used for individuals with neuromuscular disorders that yields numerous physiological and psychological benefits [1]–[4]. FES-induced rehabilitation is considered safe (i.e., noninvasive) and accessible. Some technical challenges that arise in FES-induced rehabilitation include nonphysiological muscle recruitment, variability in muscle properties between participants, muscle fatigue, and changing muscle geometry during exercises [5]. Moreover, the muscle dynamics exhibit nonlinear behavior and have unstructured uncertainty [6]. Hence, further development of closed-loop methods to produce more precise, efficient, and coordinated movements may greatly improve FES-based rehabilitative treatments [7].

To compensate for unknown nonlinear models, results such as [8]–[13] developed nonlinear robust control techniques; however, such methods rely on high-gain or high-frequency feedback to overcome the model uncertainty, which can lead to over stimulation. Motivated to remove the high-gain feedback components in FES controllers, results such as [6], [14]–[20] use neural networks (NNs) to improve performance. Rather than relying on feedback to dominate the uncertain dynamics based on worst-case results, NN-based adaptive controllers include a feedforward that adjusts to model uncertainty. However, results in [6], [14]–[20]

Emily J. Griffis, Duc M. Le, Kimberly J. Stubbs, and Warren E. Dixon are with the Department of Mechanical and Aerospace Engineering, University of Florida, Gainesville, FL, 32611–6250 USA. Email: {emilygriffis00, ledan50, kimberlyjstubbs, wdixon}@ufl.edu.

This research is supported in part by NSF award number 1762829 and by the Assistant Secretary of Defense for Health Affairs, through the Congressionally Directed Medical Research Program under Award No. W81XWH1910330. Any opinions, findings and conclusions or recommendations expressed in this material are those of the author(s) and do not necessarily reflect the views of the sponsoring agencies.

consider shallow NNs (i.e. NNs containing a single hiddenlayer).

Evidence indicates that deep neural networks (DNNs) can potentially improve function approximation because of the more complex connections and dependencies of the nonlinear activation functions [21] and [22]. Although some empirical evidence indicates improved performance over traditional shallow NNs, the complex nonlinear functionals associated with DNNs inhibit the ability to develop stability analysis driven adaptation laws and derive stability results, which limits their use in safety-critical applications such as closedloop FES control. Recent results in [23]-[26] developed a data-driven DNN-based control architecture to compensate for model uncertainty. A gradient descent-based adaptive update law is used to estimate the DNN's ideal output-layer weights continuously in real-time while an iterative datadriven method is used to adjust the inner-layer DNN weights. The results in [23]-[25] consider linear systems with known system matrices, and the extension in [26] guarantees asymptotic tracking of a desired trajectory for general control-affine nonlinear systems with model uncertainty.

This paper leverages the developments in [26] to develop a data-driven DNN-based adaptive controller for closedloop FES-induced lower-limb trajectory tracking. Unlike the results in [26], a more complex, uncertain Euler-Lagrange model is considered for the lower-limb model dynamics. The developed DNN architecture updates the output-layer DNN weights online (in real-time) while integrating data-driven methods to adjust the inner-layer DNN weights for improved controller performance. Upon initialization, the inner-layer weights may be randomly selected or obtained a priori from DNN training algorithms. Moreover, data may be collected and DNN training algorithms may be used to selectively tune the inner-layer DNN weights concurrent to real-time execution. This enables the controller to compensate for each participant's unique dynamic model and physical attributes (e.g., muscular response to FES varies between participants). To account for switching from iterative updates of the DNN weights, a nonsmooth Lyapunov-based stability analysis is used to guarantee semi-global asymptotic tracking of a desired trajectory.

This paper is structured as follows. Section II introduces the lower-limb model dynamics. Section III details the control objective, DNN-based feedforward adaptive control laws, and the developed closed-loop error system. The closed-loop error system is analyzed with a nonsmooth Lyapunov-like stability analysis in Section IV.

#### II. DYNAMICS

The nonlinear, unknown leg extension dynamics can be modeled as [27] and [28]

$$M(\ddot{q}) + P(q) + G(q) + V(\dot{q}) + \tau_d(t) = \tau(q, \dot{q}, t),$$
 (1)

where  $q:\mathbb{R}_{\geq 0} \to \mathcal{Q}, \ \dot{q}:\mathbb{R}_{\geq 0} \to \mathbb{R}$ , and  $\ddot{q}:\mathbb{R}_{\geq 0} \to \mathbb{R}$  denote the angular position (see Fig. 1), velocity, and acceleration of the shank about the knee-joint, respectively;  $\mathcal{Q} \subseteq \mathbb{R}$  denotes the set of all possible knee-joint angles. The states q and  $\dot{q}$  are both assumed to be measurable. The inertial, gravitational, and viscous damping effects are denoted by  $M:\mathbb{R}\to\mathbb{R}$ ,  $G:\mathcal{Q}\to\mathbb{R}$ , and  $V:\mathbb{R}\to\mathbb{R}$ , respectively, and the participant's passive viscoelastic tissue effects are denoted by  $P:\mathcal{Q}\to\mathbb{R}$ . Unmodeled bounded disturbances are denoted by  $T:\mathbb{R}\to\mathbb{R}$  and  $T:\mathbb{R}\to\mathbb{R}$  and  $T:\mathbb{R}\to\mathbb{R}$  are denoted by  $T:\mathbb{R}\to\mathbb{R}$ . The knee-joint torque produced due to FES stimulation is denoted by  $T:\mathbb{R}\to\mathbb{R}$ . The effects of inertia and gravity can be modeled as

$$M\left(\ddot{q}\right) = J\ddot{q},\tag{2}$$

$$G(q) = mgl\sin(q), \tag{3}$$

respectively, where  $J \in \mathbb{R}_{>0}$  denotes the unknown moment of inertia of the shank,  $m \in \mathbb{R}_{>0}$  denotes the unknown mass of the lower limb,  $l \in \mathbb{R}_{>0}$  denotes the unknown length between the knee-joint and center of mass of the shank, and  $g \in \mathbb{R}_{>0}$  denotes the gravitational acceleration constant. The passive viscoelastic tissue effects are modeled as [29]

$$P(q) = -k_1 (\exp(-k_2 q)) (q - k_3), \tag{4}$$

where  $k_1, k_2, k_3 \in \mathbb{R}_{>0}$  are unknown constants. The viscous damping effects are modeled as [27]

$$V(\dot{q}) = B_1 \tanh(-B_2 \dot{q}) - B_3 \dot{q},$$
 (5)

where  $B_1, B_2, B_3 \in \mathbb{R}_{>0}$  are unknown constants. The knee input torque can be modeled using the muscle tendon forces  $F: \mathcal{Q} \times \mathbb{R} \times \mathbb{R}_{\geq 0} \to \mathbb{R}$  and the moment arm  $\xi: \mathcal{Q} \to \mathbb{R}$ . The torque produced about the knee-joint is modeled as [30] and [31]

$$\tau\left(q,\dot{q},t\right) = \xi\left(q\right)F\left(q,\dot{q},t\right),\tag{6}$$

and the muscle tendon forces are modeled as

$$F(q, \dot{q}, t) = \eta(q, \dot{q}) u(t), \qquad (7)$$

where  $\eta:\mathcal{Q}\times\mathbb{R}\to\mathbb{R}$  denotes an unknown nonlinear function representing muscle efficiency, and  $u:\mathbb{R}_{\geq 0}\to\mathbb{R}$  denotes the FES control input to the quadriceps muscle group. To facilitate the subsequent control development, an auxiliary function  $\Omega:\mathcal{Q}\times\mathbb{R}\to\mathbb{R}_{>0}$  is defined as

$$\Omega\left(q,\dot{q}\right) \triangleq \xi\left(q\right)\eta\left(q,\dot{q}\right). \tag{8}$$

The following property and assumptions facilitate the subsequent stability analysis.

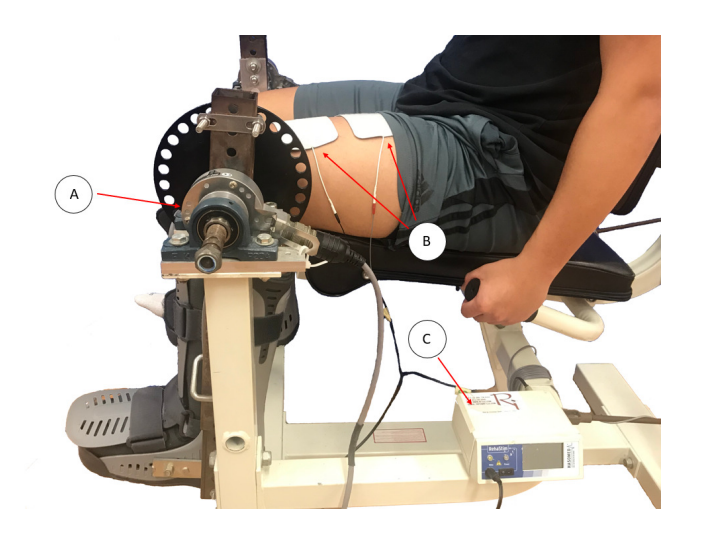


Fig. 1. Illustration of the lower-limb dynamic system with (a) an encoder at the knee-joint, (b) external electrodes placed on the participant's quadriceps, and (c) an FES stimulator.

**Property 1.** The moment of inertia J can be bounded such that  $J \leq \overline{J}$ , where  $\overline{J} \in \mathbb{R}_{>0}$  is a known constant [6] and [32].

**Assumption 1.** The torque disturbance  $\tau_d(t)$  can be bounded such that  $|\tau_d(t)| \leq \overline{\tau_d}$  for all time  $t \in \mathbb{R}_{\geq 0}$ , where  $\overline{\tau_d} \in \mathbb{R}_{> 0}$  is a known constant [6], [28], [32].

**Assumption 2.** The moment arm  $\xi\left(q\right)$  can be upper and lower bounded such that  $\underline{\xi} \leq \xi\left(q\right) \leq \overline{\xi}$  for all  $q \in \mathcal{Q}$ , where  $\underline{\xi}, \overline{\xi} \in \mathbb{R}_{>0}$  are known constants. The time derivative of  $\xi\left(q\right)$  is denoted by  $\dot{\xi}: \mathcal{Q} \to \mathbb{R}$ , and is assumed to exist and can be bounded such that  $\left|\dot{\xi}\left(q\right)\right| \leq \overline{\dot{\xi}}$  for all  $q \in \mathcal{Q}$ , where  $\overline{\dot{\xi}} \in \mathbb{R}_{>0}$  is a known constant [6], [28], [30]–[33].

**Assumption 3.** The function  $\eta\left(q,\dot{q}\right)$  can be upper and lower bounded such that  $\underline{\eta} \leq \eta\left(q,\dot{q}\right) \leq \overline{\eta}$  for all  $q \in \mathcal{Q}$  and  $\dot{q} \in \mathbb{R}$ , where  $\underline{\eta}, \overline{\eta} \in \mathbb{R}_{>0}$  are known constants. Based on empirical data, the time derivative of  $\eta(q,\dot{q})$  is denoted by  $\dot{\eta}: \mathcal{Q} \times \mathbb{R} \to \mathbb{R}$ , and is assumed to exist and can be bounded such that  $|\dot{\eta}\left(q\right)| \leq \overline{\dot{\eta}}$  for all  $q \in \mathcal{Q}$  and  $\dot{q} \in \mathbb{R}$ , where  $\overline{\dot{\eta}} \in \mathbb{R}_{>0}$  is a known constant [6], [32], [34].

### III. CONTROL DESIGN

The control objective is to design an adaptive DNN-based FES controller that ensures the knee-joint angle tracks a user-defined desired trajectory. To quantify the tracking objective, the position tracking error  $e: \mathbb{R}_{\geq 0} \to \mathbb{R}$  is defined as

$$e(t) \triangleq q_d(t) - q(t), \tag{9}$$

where  $q_d: \mathbb{R}_{\geq 0} \to \mathbb{R}$  denotes a user-defined desired angular position and is designed to be sufficiently smooth, i.e., the desired trajectory and its first two time derivatives can be bounded as  $|q_d(t)| \leq \overline{q_d}$ ,  $|\dot{q}_d(t)| \leq \overline{\dot{q}_d}$ , and  $|\ddot{q}_d(t)| \leq \overline{\ddot{q}_d}$  for all  $t \in \mathbb{R}_{\geq 0}$ , where  $\overline{q_d}$ ,  $\dot{q}_d$ ,  $\dot{\overline{q}_d} \in \mathbb{R}_{\geq 0}$  are known constants. An auxiliary tracking error  $r: \mathbb{R}_{>0} \to \mathbb{R}$  is defined as

$$r(t) \triangleq \dot{e}(t) + \alpha e(t),$$
 (10)

where  $\alpha \in \mathbb{R}_{>0}$  is a user-selected constant control parameter.

## A. Open-Loop Error System Development

Using (6)–(8), the dynamics in (1) can be rewritten as<sup>1</sup>

$$J\ddot{q} + P + G + V + \tau_d = \Omega u. \tag{11}$$

To facilitate the subsequent control development, let  $J_\Omega: \mathcal{Q} \times \mathbb{R} \to \mathbb{R}_{>0}$  be defined as  $J_\Omega\left(q,\dot{q}\right) \triangleq \frac{J}{\Omega}$ . Note that by Property 1 and Assumptions 2 and 3, the auxiliary function  $\Omega\left(q,\dot{q}\right)$  and the time derivative of  $J_\Omega\left(q,\dot{q}\right)$  are bounded such that  $|\Omega\left(q,\dot{q}\right)| \geq \Omega > 0$  and  $\left|\dot{J}_\Omega\left(q,\dot{q}\right)\right| \leq \overline{\dot{J}}_\Omega$  for all  $q \in \mathcal{Q}$  and  $\dot{q} \in \mathbb{R}$ , where  $\Omega \in \mathbb{R}_{>0}$  and  $\dot{J}_\Omega \in \mathbb{R}$  are known constants. Let the unknown model dynamics  $f: \mathcal{Q} \times \mathbb{R} \to \mathbb{R}$  be defined

$$f(x) \triangleq \frac{1}{\Omega} (P + G + V),$$
 (12)

where  $x: \mathbb{R}_{\geq 0} \to \mathcal{Q} \times \mathbb{R}$  denotes a concatenated state and is defined as  $x \triangleq [q, \dot{q}]^T$ . Taking the time derivative of (10), pre-multiplying by  $J_{\Omega}$ , and using (1), (9), and (12) yields the open-loop error system

$$J_{\Omega}\dot{r} = J_{\Omega}\ddot{q}_d - u + f(x) + \frac{1}{\Omega}\tau_d + \alpha J_{\Omega}\dot{e}.$$
 (13)

### B. Feedforward DNN Estimate

Because the dynamic model in (13) does not adhere to the typical linear-in-uncertain-parameters assumption, a DNN-based feedforward estimate is developed in this section. Let  $\Theta \subset \mathcal{Q} \times \mathbb{R}$  be a compact simply connected set, and let  $\mathbb{C} (\Theta)$  denote the space where  $f(x) \in \mathbb{C} (\Theta)$  is continuous. The Stone-Weierstrass theorem states there exists ideal weights and basis functions such that the function  $f(x) \in \mathbb{C} (\Theta)$  can be represented as [35]

$$f(x) = W^{*T} \sigma^* \left( \Phi^* \left( x \right) \right) + \varepsilon \left( x \right), \tag{14}$$

where  $W^* \in \mathbb{R}^p$  denotes the unknown ideal output-layer weights of the DNN,  $\sigma^* : \mathbb{R}^L \to \mathbb{R}^p$  denotes the unknown vector of ideal activation functions corresponding to the output-layer of the DNN,  $L \in \mathbb{Z}_{\geq 0}$  denotes the user-defined number of neurons used on the output-layer,  $\varepsilon : \Theta \to \mathbb{R}$  denotes the unknown function reconstruction error, and  $\Phi^* : \Theta \to \mathbb{R}^L$  denotes the inner-layers of the DNN. The inner-layers of the DNN  $\Phi^*$  can be expressed as<sup>2</sup>

$$\Phi^*(x) = \left(W_k^{*T} \phi_k^* \circ W_{k-1}^{*T} \phi_{k-1}^* \circ \dots \circ W_1^{*T} \phi_1^*\right)(x), (15)$$

where  $k \in \mathbb{Z}$  denotes the user-defined number of inner-layers of the DNN, and for all  $j \in \{1,\ldots,k\}$ ,  $W_j^* \in \mathbb{R}^{L_j \times L_{j+1}}$  and  $\phi_j^* : \mathbb{R}^{L_j} \to \mathbb{R}^{L_j}$  denote the  $j^{th}$  inner-layer ideal weight matrix and vector of activation functions, respectively. The user-defined parameter  $L_j$  for all  $j \in \{1,\ldots,k\}$  denotes the number of neurons used in each layer. For the dynamics in

(13) and (14),  $L_1=2$  and  $L_{k+1}=L$ . Based on (14), the DNN feedforward estimate  $\hat{f}_i:\mathbb{R}^n\to\mathbb{R}^n$  is defined as

$$\hat{f}_{i}\left(x\right) \triangleq \hat{W}^{T}\left(t\right)\hat{\sigma}_{i}\left(\hat{\Phi}_{i}\left(x\right)\right),\tag{16}$$

where  $\hat{W}: \mathbb{R}_{\geq 0} \to \mathbb{R}^p$  denotes the estimated output-layer weights of the DNN,  $\hat{\sigma}_i: \mathbb{R}^L \to \mathbb{R}^p$  denotes the user-selected vector of activation functions, and  $\hat{\Phi}_i: \mathcal{Q} \times \mathbb{R} \to \mathbb{R}^L$  denotes the estimated inner-layer of the DNN. The output-layer weight estimate  $\hat{W}$  is continuously updated in real-time, and is subsequently designed. The estimated inner-layer of the DNN  $\hat{\Phi}_i$  is defined as

$$\hat{\Phi}_{i}\left(x\right) \triangleq \left(\hat{W}_{i,k}^{T} \hat{\phi}_{i,k} \circ \hat{W}_{i,k-1}^{T} \hat{\phi}_{i,k-1} \circ \dots \circ \hat{W}_{i,1}^{T} \hat{\phi}_{i,1}\right)\left(x\right),\tag{17}$$

where  $k \in \mathbb{Z}$  denotes the user-defined number of inner-layers of the DNN, and for all  $j \in \{1,\dots,k\}$ ,  $\hat{W}_{i,j}: \mathbb{Z}_{\geq 0} \to \mathbb{R}^{L_j \times L_{j+1}}$  and  $\hat{\phi}_{i,j}: \mathbb{R}^{L_j} \to \mathbb{R}^{L_j}$  denote the  $j^{th}$  inner-layer weight matrix estimate and vector of activation functions, respectively. The index i for all  $i \in \mathbb{Z}_{\geq 0}$  denotes the  $i^{th}$  iteration of training, and the initial index i = 0 corresponds to the DNN at the initial condition.

An iterative data-driven approach can be used to update the inner-layer weights of the DNN estimate in (17). Concurrent to real-time execution, data is collected and the inner-layer weight estimates are held constant until updated. DNN training algorithms such as gradient descent variants (c.f. [23]–[25], and [36, Ch. 8]) are employed on the collected data sets to update the inner-layer DNN weights. The developed DNN-based control architecture in [26] provides flexibility in the inner-layer DNN weight training process. The initialized DNN  $\hat{\Phi}_0$  can be trained *a priori* from existing data sets (i.e., data collected on able-bodied or neurologically impaired participants). Moreover, in the absence of training data sets,  $\hat{\Phi}_0$  can be initialized with random inner-layer DNN weights.

To facilitate the subsequent stability analysis, the following assumption is made.

**Assumption 4.** There exists known constants  $\overline{W^*}, \overline{\sigma^*}, \widehat{\overline{\sigma}}, \overline{\varepsilon} \in \mathbb{R}_{\geq 0}$  such that the ideal output-layer weights  $W^*$ , the ideal vector of activation functions  $\sigma^*$  (·), the user-selected vector of activation functions  $\widehat{\sigma}_i$  (·), and the function reconstruction error  $\varepsilon$  (·) can be upper bounded as  $\sup_{x \in \Theta} \|W^*\| \leq \overline{W^*}$ ,  $\sup_{x \in \Theta} \|\sigma^*$  (·) $\| \leq \overline{\sigma^*}$ ,  $\sup_{x \in \Theta, \forall i} \|\widehat{\sigma}_i$  (·) $\| \leq \overline{\widehat{\sigma}}$ , and  $\sup_{x \in \Theta} \|\varepsilon$  (·) $\| \leq \overline{\varepsilon}$ , respectively [37].

# C. Control Design

Based on the subsequent stability analysis, the FES control input is designed as

$$u \triangleq \hat{f}_i + k_r r + k_s \operatorname{sgn}(r) + e, \tag{18}$$

where  $\operatorname{sgn}(\cdot)$  denotes the signum function and  $k_r, k_s \in \mathbb{R}_{>0}$  are user-defined constant control parameters. Based on the

<sup>&</sup>lt;sup>1</sup>For notational brevity, all functional dependence on system states and time are hereafter suppressed unless required for clarity of exposition.

<sup>&</sup>lt;sup>2</sup>The symbol ∘ denotes function composition.

<sup>&</sup>lt;sup>3</sup>For some common activation functions, e.g., hyperbolic tangent functions, sigmoid functions, radial basis functions,  $\overline{\sigma^*} = \hat{\overline{\sigma}} = L$ .

subsequent stability analysis, the weight update law  $\hat{W}:\mathbb{R}_{\geq 0}\to\mathbb{R}^p$  is defined as

$$\dot{\hat{W}} \triangleq \Gamma_W \hat{\sigma}_i \left( \hat{\Phi}_i \left( x \right) \right) r, \tag{19}$$

where  $\Gamma_W \in \mathbb{R}^{p \times p}$  denotes a user-defined positive definite control gain matrix. Substituting (14), (16), and (18) into (13) yields the closed-loop error system

$$J_{\Omega}\dot{r} = -\hat{W}^{T}\hat{\sigma}_{i}\left(\hat{\Phi}_{i}\left(x\right)\right) - k_{r}r - k_{s}\operatorname{sgn}(r) + \varepsilon\left(x\right) - e$$
$$+ W^{*T}\sigma^{*}\left(\Phi^{*}\left(x\right)\right) + J_{\Omega}\ddot{q}_{d} + \frac{1}{\Omega}\tau_{d} + \alpha J_{\Omega}\dot{e}. \quad (20)$$

Guidance from the subsequent stability analysis indicates that the control gains  $k_r$  and  $k_s$  have to be selected sufficiently large, and the gain condition  $\alpha$  has to be selected sufficiently small. Specifically,  $k_r$ ,  $k_s$ , and  $\alpha$  should be selected to satisfy the sufficient gain conditions

$$k_s > \overline{W^*} \left( \overline{\sigma^*} + \overline{\hat{\sigma}} \right) + \frac{\overline{J}}{\Omega} \overline{\ddot{q}}_d + \overline{\varepsilon} + \frac{\overline{\tau_d}}{\Omega},$$
 (21)

$$k_r > \frac{1}{2}\overline{\dot{J}_{\Omega}} + \alpha \frac{\overline{J}}{\Omega} + \frac{\alpha^2}{2}\frac{\overline{J}}{\Omega},$$
 (22)

$$0 < \alpha < 2 \frac{\Omega}{\overline{I}}. \tag{23}$$

#### IV. STABILITY ANALYSIS

**Theorem 1.** Consider a system modeled by the dynamics in (1) with initial condition  $[q(0), \dot{q}(0)]^T \in \Theta$ . Let Property 1 and Assumptions 1–4 hold. The FES control input in (18) and output-layer weight adaptation law in (19) yield semiglobal asymptotic tracking in the sense that  $\lim_{t\to\infty} |e(t)| = 0$  and  $\lim_{t\to\infty} |r(t)| = 0$ , provided the sufficient gain conditions in (21)–(23) are satisfied.

*Proof*: Let  $V_L:\mathbb{R}^{2+p}\times\mathbb{R}_{\geq 0}\to\mathbb{R}$  be a candidate Lyapunov function defined as

$$V_L(z,t) \triangleq \frac{1}{2}e^2 + \frac{1}{2}J_{\Omega}r^2 + \frac{1}{2}\tilde{W}^T\Gamma_W^{-1}\tilde{W},$$
 (24)

where  $z:\mathbb{R}_{\geq 0}\to\mathbb{R}^{2+p}$  is defined as  $z\triangleq\begin{bmatrix}e,&r,&\tilde{W}^T\end{bmatrix}^T$ , and the mismatch between the ideal output-layer weights and the output-layer weight estimates  $\tilde{W}:\mathbb{R}_{\geq 0}\to\mathbb{R}^p$  are defined as

$$\tilde{W}\left(t\right) \triangleq W^* - \hat{W}\left(t\right). \tag{25}$$

Let  $\zeta: \mathbb{R}_{\geq 0} \to \mathbb{R}^{2+p}$  be a Filippov solution to the differential inclusion  $\dot{\zeta} \in K[h](\zeta,t)$ , where  $\zeta(t)=z(t)$ , the calculus of  $K[\cdot]$  is used to compute Filippov's differential inclusion as defined in [38], and  $h: \mathbb{R}^{2+p} \times \mathbb{R}_{\geq 0} \to \mathbb{R}^{2+p}$  is defined as  $h(\zeta,t) \triangleq \left[ \begin{array}{cc} \dot{e}, & \dot{r}, & \dot{W}^T \end{array} \right]^T$ . The generalized time derivative of the candidate Lyapunov function  $V_L$  along the Filippov trajectories of  $\dot{\zeta}=h(\zeta,t)$  is defined as

$$\dot{\tilde{V}}_{L}\left(\zeta,t\right) \triangleq \bigcap_{\zeta \in \partial V_{L}\left(\zeta,t\right)} \zeta^{T} \begin{bmatrix} K\left[h\right]\left(\zeta,t\right) \\ 1 \end{bmatrix}, \qquad (26)$$

where  $\partial V_L\left(\zeta,t\right)$  denotes Clarke's generalized gradient of  $V_L\left(\zeta,t\right)$  [39, Equation 22]. Since  $V_L\left(\zeta,t\right)$  is continuously differentiable in  $\zeta$ , then  $\partial V_L\left(\zeta,t\right)=\left\{\nabla V_L\left(\zeta,t\right)\right\}$ , where  $\nabla$  denotes the gradient operator. Additionally, the time derivative of  $V_L$  exists almost everywhere (a.e.), i.e.,  $\dot{V}_L\left(\zeta,t\right)\stackrel{\mathrm{a.e.}}{\in}\dot{V}_L\left(\zeta,t\right)$  for almost all  $t\in\mathbb{R}_{>0}$ .

Taking the generalized time derivative of (24) yields

$$\dot{\tilde{V}}_{L} \subseteq \left[ \begin{array}{ccc} e, & J_{\Omega}r, & \tilde{W}^{T}\Gamma_{W}^{-1}, & \frac{1}{2}\dot{J}_{\Omega}r^{2} \end{array} \right] K \left[ \begin{array}{c} \dot{e} \\ \dot{r} \\ -\dot{\hat{W}} \\ 1 \end{array} \right]. \tag{27}$$

Substituting (10), the closed-loop error system in (20), and the output-layer weight estimate update law in (19) into (27) yields

$$\dot{\tilde{V}}_{L} \subseteq r \left( -k_{r}r - k_{s}K[\operatorname{sgn}(r)] - \hat{W}^{T}K\left[\hat{\sigma}_{i}\left(\hat{\Phi}_{i}\left(x\right)\right)\right] \right) 
+ r \left(\frac{1}{\Omega}\tau_{d} + \alpha J_{\Omega}\dot{e} + W^{*T}\sigma^{*}\left(\Phi^{*}\left(x\right)\right) + \varepsilon\left(x\right)\right) 
+ rJ_{\Omega}\ddot{q}_{d} - \tilde{W}^{T}K\left[\hat{\sigma}_{i}\left(\hat{\Phi}_{i}\left(x\right)\right)\right]r - \alpha e^{2} + \frac{1}{2}\dot{J}_{\Omega}r^{2}.$$
(28)

By Property 1 and Assumptions 1–4, using Young's inequality, and adding and subtracting  $W^{*T}K\left[\hat{\sigma}_{i}\left(\hat{\Phi}_{i}\left(x\right)\right)\right]$ , the inequality in (28) can be upper bounded as

$$\dot{V}_{L} \stackrel{\text{a.e.}}{\leq} -\left(\alpha - \frac{\alpha^{2}\overline{J}}{2\underline{\Omega}}\right) e^{2} - \left(k_{r} - \frac{\overline{j_{\Omega}}}{2} - \frac{\alpha\overline{J}}{\underline{\Omega}} - \frac{\alpha^{2}\overline{J}}{2\underline{\Omega}}\right) r^{2} \\
- |r| \left(k_{s} - \overline{W}^{*} \left(\overline{\sigma}^{*} + \overline{\hat{\sigma}}\right) - \frac{\overline{J}}{\underline{\Omega}} \overline{\ddot{q}_{d}} - \overline{\varepsilon} - \frac{\overline{\tau_{d}}}{\underline{\Omega}}\right), (29)$$

where rK[sgn(r)] = |r|. Then, provided the sufficient gain conditions in (21)–(23) are satisfied, the inequality in (29) can be upper bounded as

$$\dot{V}_L \stackrel{\text{a.e.}}{\leq} -\lambda \|y\|^2 \,, \tag{30}$$

where  $y \triangleq [e,r]^T$  denotes a concatenated state, and  $\lambda \in \mathbb{R}_{>0}$  is a known constant defined as  $\lambda \triangleq \min\left\{\alpha - \frac{\alpha^2}{2}\frac{\overline{J}}{\underline{\Omega}}, k_r - \frac{1}{2}\frac{\overline{J}}{\overline{\Omega}} - \alpha\frac{\overline{J}}{\underline{\Omega}} - \frac{\alpha^2}{2}\frac{\overline{J}}{\underline{\Omega}}\right\}$ .

From (24) and (30),  $V_L$  is positive semi-definite and non-increasing, which implies  $V_L \in \mathcal{L}_{\infty}$ , and hence,  $z \in \mathcal{L}_{\infty}$ . Since  $z \in \mathcal{L}_{\infty}$ , this implies  $e, r, \tilde{W} \in \mathcal{L}_{\infty}$ . Using (9), (10), and (25), the fact that  $e, r, \tilde{W} \in \mathcal{L}_{\infty}$  implies  $q, \dot{q}, \dot{e}, \hat{W} \in \mathcal{L}_{\infty}$ . By Assumption 4,  $\hat{\sigma}_i \in \mathcal{L}_{\infty}$ . Using (19), the fact that  $\hat{\sigma}_i, r \in \mathcal{L}_{\infty}$  implies the output-layer weight estimate update law  $\hat{W} \in \mathcal{L}_{\infty}$ . Since  $\ddot{q}_d \in \mathcal{L}_{\infty}$  by design, the fact that  $e, r, \hat{W}, \hat{\sigma} \in \mathcal{L}_{\infty}$  implies the control input  $u \in \mathcal{L}_{\infty}$ . By the LaSalle-Yoshizawa extension for nonsmooth systems in [40],  $\lambda \|y\|^2 \to 0$  as  $t \to \infty$ , which implies  $\lim_{t \to \infty} |e(t)| = 0$  and  $\lim_{t \to \infty} |r(t)| = 0$ .

#### V. CONCLUSIONS

This paper uses Lyapunov-based methods to develop a data-driven DNN-based adaptive control method for FESinduced leg extension rehabilitation. The developed DNN architecture updates the output-layer DNN weights online (in real-time) while integrating data-driven methods to update the inner-layer DNN weights for improved controller performance. To account for switching from iterative updates of the inner-layer DNN weights, a nonsmooth Lyapunovbased stability analysis is used to guarantee semi-global asymptotic tracking of a desired trajectory. Future research efforts include experimental studies with neurologically impaired participants and extending the developed DNN-based adaptive control architecture to switched system models, which will enable more precise coordination and activation of multiple muscle groups for more complex exercises (e.g., FES-induced cycling).

#### REFERENCES

- [1] P. H. Peckham and D. B. Gray, "Functional neuromuscular stimulation," *J. Rehabil. Res. Dev.*, vol. 33, pp. 9–11, 1996.
- [2] T. Yan, C. W. Y. Hui-Chan, and L. S. W. Li, "Functional electrical stimulation improves motor recovery of the lower extremity and walking ability of subjects with first acute stroke: A randomized placebo-controlled trial," *Stroke*, vol. 36, no. 1, pp. 80–85, 2005.
- [3] P. H. Peckham, "Functional electrical stimulation: current status and future prospects of applications to the neuromuscular system in spinal cord injury," *Paraplegia*, vol. 25, pp. 279–288, June 1987.
- [4] A. Kralj and T. Bajd, Functional electrical stimulation: standing and walking after spinal cord injury. CRC, 1989.
- [5] K. J. Hunt, J. Fang, J. Saengsuwan, M. Grob, and M. Laubacher, "On the efficiency of FES cycling: A framework and systematic review," *Technol. Health Care*, vol. 20, no. 5, pp. 395–422, 2012.
- [6] N. Sharma, C. M. Gregory, M. Johnson, and W. E. Dixon, "Closed-loop neural network-based nmes control for human limb tracking," *IEEE Trans. Control Syst. Tech.*, vol. 20, no. 3, pp. 712–725, 2012.
- [7] C. T. Freeman, E. Rogers, A.-M. Hughes, J. H. Burridge, and K. L. Meadmore, "Iterative learning control in health care: Electrical stimulation and robotic-assisted upper-limb stroke rehabilitation," *IEEE Control Syst. Mag.*, vol. 32, pp. 18–43, Feb. 2012.
- [8] S. Jezernik, R. G. V. Wassink, and T. Keller, "Sliding mode closed-loop control of fes controlling the shank movement," *IEEE Trans. Biomed. Eng.*, vol. 51, no. 2, pp. 263–272, 2004.
- [9] M. J. Bellman, T. H. Cheng, R. J. Downey, C. J. Hass, and W. E. Dixon, "Switched control of cadence during stationary cycling induced by functional electrical stimulation," *IEEE Trans. Neural Syst. Rehabil. Eng.*, vol. 24, no. 12, pp. 1373–1383, 2016.
- [10] N. Sharma, K. Stegath, C. M. Gregory, and W. E. Dixon, "Nonlinear neuromuscular electrical stimulation tracking control of a human limb," *IEEE Trans. Neural Syst. Rehabil. Eng.*, vol. 17, pp. 576–584, Jun. 2009.
- [11] N. Sharma, S. Bhasin, Q. Wang, and W. E. Dixon, "RISE-based adaptive control of a control affine uncertain nonlinear system with unknown state delays," *IEEE Trans. Autom. Control*, vol. 57, pp. 255– 259, Jan. 2012.
- [12] N. Sharma, C. M. Gregory, M. Johnson, and W. E. Dixon, "Modified neural network-based electrical stimulation for human limb tracking," in *Proc. IEEE Int. Symp. Intell. Control*, (San Antonio, Texas), pp. 1320–1325, Sep. 2008.
- [13] S. Bhasin, N. Sharma, P. Patre, and W. E. Dixon, "Robust asymptotic tracking of a class of nonlinear systems using an adaptive critic based controller," in *Proc. Am. Control Conf.*, (Baltimore, MD), pp. 3223– 3228, 2010.
- [14] Y. Li, W. Chen, J. Chen, X. Chen, J. Liang, and M. Du, "Neural network based modeling and control of elbow joint motion under functional electrical stimulation," *Neurocomputing*, vol. 340, pp. 171– 179, 2019.

- [15] G.-C. Chang, J.-J. Lub, G.-D. Liao, J.-S. Lai, C.-K. Cheng, B.-L. Kuo, and T.-S. Kuo, "A neuro-control system for the knee joint position control with quadriceps stimulation," *IEEE Trans. Rehabil. Eng.*, vol. 5, pp. 2–11, Mar. 1997.
- [16] H. Y. Zhou, L. K. Huang, Y. M. Gao, Z. L. Vasic, M. Cifrek, and M. Du, "Estimating the ankle angle induced by fes via the neural network-based hammerstein model," *IEEE Access*, vol. 7, pp. 141277– 141286, 2019.
- [17] J. J. Abbas and H. J. Chizeck, "Neural network control of functional neuromuscular stimulation systems: computer simulation studies," *IEEE Trans. Biomed. Eng.*, vol. 42, pp. 1117–1127, Nov. 1995.
- [18] N. Lan, H.-Q. Feng, and P. E. Crago, "Neural network generation of muscle stimulation patterns for control of arm movements," *IEEE Trans. Rehabil. Eng.*, vol. 2, pp. 213–224, Dec. 1994.
- [19] D. Graupe and H. Kordylewski, "Artificial neural network control of FES in paraplegics for patient responsive ambulation," *IEEE Trans. Biomed. Eng.*, vol. 42, pp. 699–707, July 1995.
- [20] H. Kordylewski and D. Graupe, "Control of neuromuscular stimulation for ambulation by complete paraplegics via artificial neural networks," *Neurol. Res.*, vol. 23, pp. 472–481, July 2001.
- [21] Y. LeCun, Y. Bengio, and G. Hinton, "Deep learning," *Nature*, vol. 521, no. 7553, pp. 436–444, 2015.
- [22] Q. Teng and L. Zhanga, "Data driven nonlinear dynamical systems identication using multi-step CLDNN," AIP Advances, 2019.
- [23] G. Joshi, J. Virdi, and G. Chowdhary, "Design and flight evaluation of deep model reference adaptive controller," in AIAA Scitech 2020 Forum, p. 1336, 2020.
- [24] G. Joshi and G. Chowdhary, "Deep model reference adaptive control," in *IEEE Conf. Decis. Control*, pp. 4601–4608, IEEE, 2019.
- [25] G. Joshi, J. Virdi, and G. Chowdhary, "Asynchronous deep model reference adaptive control," *Proc. PMLR Conf. Robot Learn.*, pp. 4601–4608. November 2020.
- [26] R. Sun, M. Greene, D. Le, Z. Bell, G. Chowdhary, and W. E. Dixon, "Lyapunov-based real-time and iterative adjustment of deep neural networks," *IEEE Control Syst. Lett.*, vol. 6, pp. 193–198, 2021.
- [27] T. Schauer, N. O. Negård, F. Previdi, K. J. Hunt, M. H. Fraser, E. Ferchland, and J. Raisch, "Online identification and nonlinear control of the electrically stimulated quadriceps muscle," *Control Eng. Pract.*, vol. 13, pp. 1207–1219, Sept. 2005.
- [28] L. Cheng, Y. Wang, W. Ren, Z.-G. Hou, and M. Tan, "On convergence rate of leader-following consensus of linear multi-agent systems with communication noises," *IEEE Trans. Autom. Control*, vol. 61, no. 11, pp. 3586–3592, 2016.
- [29] M. Ferrarin and A. Pedotti, "The relationship between electrical stimulus and joint torque: A dynamic model," *IEEE Trans. Rehabil. Eng.*, vol. 8, pp. 342–352, Sept. 2000.
- [30] J. L. Krevolin, M. G. Pandy, and J. C. Pearce, "Moment arm of the patellar tendon in the human knee," *J. Biomech.*, vol. 37, no. 5, pp. 785–788, 2004.
- [31] W. L. Buford, J. F. M. Ivey, J. D. Malone, R. M. Patterson, G. L. Peare, D. K. Nguyen, and A. A. Stewart, "Muscle balance at the knee moment arms for the normal knee and the ACL minus knee," *IEEE Trans. Rehabil. Eng.*, vol. 5, pp. 367–379, Dec. 1997.
- [32] R. J. Downey, T.-H. Cheng, M. J. Bellman, and W. E. Dixon, "Switched tracking control of the lower limb during asynchronous neuromuscular electrical stimulation: Theory and experiments," *IEEE Trans. Cybern.*, vol. 47, pp. 1251–1262, May 2017.
- [33] R. Nathan and M. Tavi, "The influence of stimulation pulse frequency on the generation of joint moments in the upper limb," *IEEE Trans. Biomed. Eng.*, vol. 37, pp. 317–322, Mar. 1990.
- [34] Y. Giat, J. Mizrahi, and M. Levy, "A musculotendon model of the fatigue profiles of paralyzed quadriceps muscle under FES," *IEEE Trans. Biomed. Eng.*, vol. 40, pp. 664–674, July 1993.
- [35] N. E. Cotter, "The stone-weierstrass theorem and its application to neural networks," *IEEE Trans. Neural Netw.*, vol. 1, no. 4, pp. 290– 295, 1990.
- [36] I. Goodfellow, Y. Bengio, A. Courville, and Y. Bengio, *Deep learning*, vol. 1. MIT press Cambridge, 2016.
- [37] F. L. Lewis, S. Jagannathan, and A. Yesildirak, Neural network control of robot manipulators and nonlinear systems. Philadelphia, PA: CRC Press. 1998.
- [38] B. E. Paden and S. S. Sastry, "A calculus for computing Filippov's differential inclusion with application to the variable structure control

- of robot manipulators," *IEEE Trans. Circuits Syst.*, vol. 34, pp. 73–82, Ian 1987
- [39] D. Shevitz and B. Paden, "Lyapunov stability theory of nonsmooth systems," *IEEE Trans. Autom. Control*, vol. 39 no. 9, pp. 1910–1914, 1994.
- [40] R. Kamalapurkar, J. A. Rosenfeld, A. Parikh, A. R. Teel, and W. E. Dixon, "Invariance-like results for nonautonomous switched systems," *IEEE Trans. Autom. Control*, vol. 64, pp. 614–627, Feb. 2019.